

Lateral photovoltaic effect in the $\text{Fe}_3\text{O}_4/\text{SiO}_2/n\text{-Si}$ structure: influence of the SiO_2 thickness

© T.A. Pisarenko,¹ D.A. Tsukanov,^{1,2} V.V. Balashev,^{1,2} A.A. Yakovlev¹

¹Institute of Automation and Control Processes, Far East Branch, Russian Academy of Sciences, 690014 Vladivostok, Russia

²Far Eastern Federal University, 690922 Vladivostok, Russia
e-mail: tata_dvo@iacp.dvo.ru

Received April 22, 2024

Revised December 20, 2024

Accepted February 18, 2025.

The work provides research on the lateral photovoltaic effect in the $\text{Fe}_3\text{O}_4/\text{SiO}_2/n\text{-Si}$ structure with the thickness of the silicon oxide layer 2 and 5 nm. It has been shown that increase of the thickness of the SiO_2 layer in the studied structure results in a changed type of dependences of sensitivity and nonlinearity of lateral photovoltage on the thickness of the Fe_3O_4 film as well as a form of photoresponse signals under pulsed illumination. It has been established that a change of photosensitivity in the $\text{Fe}_3\text{O}_4/\text{SiO}_2/n\text{-Si}$ structure with increase of the thickness of SiO_2 is due to both influence of surface and interface states at the $\text{SiO}_2/n\text{-Si}$ interface and redistribution of channel conductivity as well. Extrema on the thickness dependence of the photovoltaic characteristics are related to the quantum-size effect which modulates a height of the built-in barrier.

Keywords: optoelectronic devices, photovoltaic effect, photoresponse, magnetite, silicon.

DOI: 10.61011/TP.2025.04.61214.138-24

Introduction

Important components of the optoelectronic devices that are widely used in various applications of industrial production, scientific research and everyday life are photovoltaic detectors based on conversion of light signals into electrical ones [1–5]. Development of nanotechnologies stimulates innovations in optoelectronics. Thus, recently, the lateral photovoltaic effect (LPE) in silicon-based hybrid structures of the $\text{Me}/\text{SiO}_2/\text{Si}$ type (Me — metal) attracts attention of researchers due to prospects of creation of position-sensitive detectors (PSD) with a continuous photovoltaic signal from large working surfaces [5–9].

It is known [1–4] that the LPE occurs under heterogeneous irradiation of a surface of the pn-junction or the quasi pn-junction induced by a thin conductive layer near the SiO_2/Si interface in the $\text{Me}/\text{SiO}_2/\text{Si}$ structure. In doing so, a large number of electron-hole pairs is excited and then separated in an illuminated place by means of the built-in field. Thus, difference of electrical potentials between the n - and p -regions is created in the illuminated region due to excessive photocarriers accumulated therein — it is a well-known transverse photovoltaic effect. As a result of non-uniform illumination, in addition to the transverse photoeffect in the illuminated region, there is also a carrier concentration gradient between the illuminated and unilluminated region, thereby resulting in lateral diffusion of the excessive photocarriers from the illuminated place to contacts [1–3]. At the same time, it is interesting to note the fact that the lateral diffusion process does not depend on the external field, thereby meaning large

prospects of LPE application in high-performance devices of optoelectronics [5,9].

The LPE has been well studied recently in various hybrid nanostructures of the metal-semiconductor (MS) type, the metal-oxide-semiconductor (MOS) type and the heterostructures [10–13]. The reviews [10–12] note high sensitivity of this effect to material properties of the upper layer: its thickness, conductivity, a ratio of work function to substrate's work function as well as to laser radiation characteristics: the wavelength and the radiation power.

Improvement of the LPE-based PSD characteristics requires deeper understanding of processes of generation and current transfer of the photogenerated carriers. We have previously shown [12] that in the hybrid structure with different conductivity of the upper layer the non-equilibrium photocarriers are generated and separated in a subsurface layer of the silicon substrate, while the current transfer mechanism is represented by a two-channel model of conductivity [14–16].

The works [10,11,13] attempt to describe the lateral photoconductivity mechanism in terms of morphological properties of the upper coating. Influence of roughness on film resistance at the initial stage of their growth and the light scattering mechanism are undoubted, but the works [10,11,13] do not provide confirmation of the theoretical considerations with any experimental data.

We have previously studied the LPE in the $\text{Fe}_3\text{O}_4/\text{SiO}_2/\text{Si}$ structure quite extensively [16–20]. Our previous works presented results of research of influence on the LPE by such parameters as the conductivity type of the silicon substrate

and the thickness of the magnetite film [17], orientation of the silicon substrate [18] and the temperature [19]. It has been found [19] that with reduction of the temperature to 122 K due to the Verwey transition [21–22] the magnetite becomes an insulator, while the LPE sensitivity decreases in two times and nonlinearity increases more than in two times. These changes were explained in terms of both changed energy parameters of the $\text{Fe}_3\text{O}_4/\text{SiO}_2/\text{Si}$ system and the two-channel model of lateral photoconductivity [12,16].

The aim of the present work is to analyze the mechanism of lateral photoconductivity in the $\text{Fe}_3\text{O}_4/\text{SiO}_2/n\text{-Si}$ structure with the different thickness of the SiO_2 layer. In order to understand the current transfer mechanism, in the present work we propose the two-channel model of lateral photoconductivity, which is characterized by redistribution of channel conductivity when changing both the thickness of the magnetite film and the thickness of the SiO_2 layer. It has been shown that parallel channels of conductivity are the film of the upper layer and the SiO_2/Si interface-adjacent thin layer of silicon, (which is an inversion layer in this case), together with near-contact tunneling regions. The maximum of LPE sensitivity in structures with an ultra-thin SiO_2 layer occurs under a condition that the homogeneous built-in barrier is formed [10,17], at which there is an optimal ratio between the electrical resistance of the film and total resistance of the inversion layer and the tunneling near-contact regions, resulting to redistribution of contributions of the conductivity channels [14,16]. With increase of the thickness of the silicon oxide layer in the $\text{Fe}_3\text{O}_4/\text{SiO}_2/n\text{-Si}$ structure, the dependence of sensitivity of lateral photovoltage on the thickness of the magnetite film exhibits two maxima which in our opinion exist due to the quantum-size effects in the magnetite film.

1. Experimental procedure

The substrates were single-crystal wafers Si(001) of the n -type, which were alloyed with phosphorous and had specific resistance of $7.5 \Omega\cdot\text{cm}$. These wafers were with the $\text{Fe}_3\text{O}_4/\text{SiO}_2/\text{Si}$ structures formed thereon by the tunnel-thin SiO_2 layers of the thickness 2 and 5 nm. For the first series of the samples, before loading the samples into a vacuum chamber, the Si substrates surface was provided with the ultra-thin SiO_2 layer of the thickness of 2 nm at the final stage of wet chemical purification in nitric acid (68 % HNO_3) at 120 °C for 10 min [23,24]. For the second series of the samples we have used silicon wafers with the SiO_2 layers of the thickness of 5 nm, which were industrially produced by the thermal oxidation method [25,26].

The magnetite films (Fe_3O_4) were formed on these substrates in an ultrahigh-vacuum (UHV) Katun chamber with the basic pressure of $2 \cdot 10^{-10}$ Torr by depositing iron at the rate of 2.5 nm/min in the oxygen atmosphere under $P_{\text{O}_2} = 10^{-6}$ Torr at the substrate temperature of 300 °C. The process of growth of the Fe_3O_4 film was observed by means of Reflection high-energy electron diffraction (RHEED). The

film thickness was controlled by spectroscopic ellipsometry directly during growth in the UHV chamber.

In order to measure photovoltage, aluminum contacts were applied by thermal vacuum sputtering to the film surface through a metal mask in the form of strips 2×1 mm with the distance of 2 mm therebetween. The electrical resistance was measured in a two-probe method using the Keithley-2000 multimeter in a mode of electrical resistance to direct current under control by current-voltage curves of the measured configuration. Illumination was provided by a He-Ne-laser (ML101J25) of the wavelength of 633 nm and an irradiation power incident on the sample surface of 0.25 mW. The diameter of the light spot was $50 \mu\text{m}$. The dependences of photovoltage $U(x)$ and $U(t)$ were measured by means of the Keithley-2000 multimeter and the Tektronix TDS 2012B digital oscilloscope, respectively.

2. Results and discussion

It is well known [1–3] that the LPE is based on transverse separation and lateral diffusion of the photogenerated carriers, whereas the lateral photovoltage heavily depends on the value of the built-in potential. There is an opinion [10] that in order to increase LPE sensitivity in the hybrid structures it is necessary to increase the electrical resistance of the upper film. In terms of the two-channel model, in which the inversion layer in the subsurface region of the Si(100) substrate and the Fe_3O_4 film form two parallel conductivity channels [12,14,16], this assumption is reasonable. It is due to the fact that as higher the film resistance the higher probability that the homogeneous built-in barrier at the SiO_2/Si interface will be formed before the film starts bypassing the inversion layer (in which the photovoltage is generated), as in the two-channel model of conductivity the film resistance shall be regarded as load resistance. However, as shown in the work [12], too high resistance of the upper layer result both in the increased lateral photovoltage and increased LPE nonlinearity as well. Thus, we think that in case of the $\text{TiO}_2/\text{SiO}_2/\text{Si}$ heterostructure, the increase of LPE sensitivity is due not to the value of resistance of the titanium dioxide film, but to the value of the built-in potential at the SiO_2/Si interface. This is why, in our view, comparison of the SiO_2 and TiO_2 buffer layers from the work [10] is insufficient for identifying and understanding the mechanism of lateral photoconductivity.

The present work proposes to clarify the mechanism of lateral photoconductivity in the $\text{Fe}_3\text{O}_4/\text{SiO}_2/n\text{-Si}$ system in a method of varying the thicknesses of the magnetite film and the silicon oxide layer.

Fig. 1 shows the dependences of lateral photovoltage (U_l) on the position of the laser spot for the $\text{Fe}_3\text{O}_4/\text{SiO}_2/n\text{-Si}$ structures which are formed on the oxidized silicon surface with the thickness of the SiO_2 layer 2 and 5 nm (Fig. 1, *a* and *b*, respectively). As can be seen in Fig. 1, the maximum value of lateral photovoltage in the structure with ultra-thin SiO_2 is ~ 4 times higher than in the structure with the

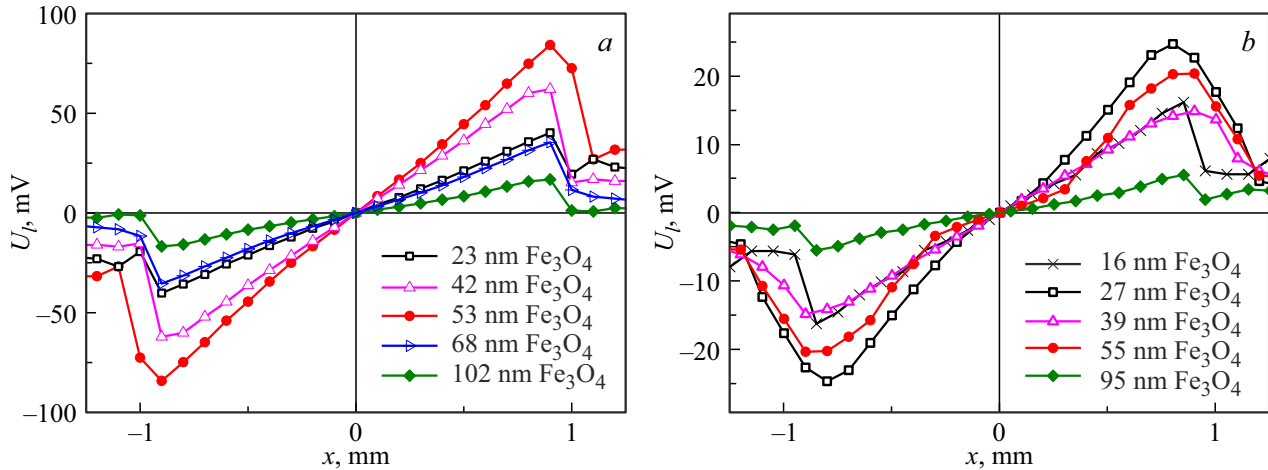


Figure 1. Dependences of the lateral photovoltage on the position of the laser spot for the $\text{Fe}_3\text{O}_4/\text{SiO}_2/n\text{-Si}$ structures with the thickness of the layer SiO_2 : *a* — 2 nm; *b* — 5 nm.

thermally oxidized thin SiO_2 layer, although in both cases in the region between the contacts the lateral photovoltage varies linearly. Such substantial difference in the value of lateral photovoltage may be related, in our opinion, to the changed height of the built-in barrier due to influence of the interface states at the $\text{SiO}_2/n\text{-Si}$ interface, as we have found previously [17]. The authors of method of chemical oxidation of silicon in nitric acid, which is used in the present work, have studied physical characteristics of the SiO_2/Si and shown that these structures are advantageous in small leakage currents caused, as the authors think, by availability of the interface states [23]. The work [23] also notes that the closest in physical characteristics to their structures are the SiO_2/Si interfaces which are produced by thermal oxidation with the oxide thickness of ~ 1.5 nm. We note that the present work uses the thermally oxidized SiO_2 layers of the thickness of 5 nm. It is known that the density of the interface states of the SiO_2/Si interface produced by chemical oxidation in nitric acid and thermal oxidation is $6.3 \cdot 10^9$ [27] and $\sim 10^{11} \text{ eV}^{-1}\text{cm}^{-2}$ [28] respectively. This difference in the density of the interface states may result in changing the height of the built-in barrier to 0.1 eV [29].

It is also clear from Fig. 1 that lateral photovoltage non-monotonically varies with increase in the thickness of the magnetite films.

The dependences of lateral photovoltage on the position of the laser spot were parameterized by the magnitudes of sensitivity (κ) and nonlinearity (δ), which are PSD working characteristics (Fig. 2). It is clear from the figure that increase of the thickness of the SiO_2 layer results in a changed nature of the dependences $\kappa(d)$ and $\delta(d)$. Thus, for the structure with the thickness of SiO_2 2 nm the dependence $\kappa(d)$ has one maximum, which is typical for the MS and MOS structures with the natural SiO_2 layer [10–13], whereas for the structure of the thickness of SiO_2 5 nm the dependence $\kappa(d)$ becomes a multi-mode one (Fig. 2, *a*).

It is clear from Fig. 2, *b* that in case of the ultra-thin SiO_2 layer the LPE nonlinearity exponentially decreases, whereas with increase of the thickness of the SiO_2 layer the dependence $\delta(d)$ is of a multi-mode nature as in the case with sensitivity.

In order to analyze the mechanism of lateral photoconductivity in the $\text{Fe}_3\text{O}_4/\text{SiO}_2/n\text{-Si}$ structure, it is necessary to remember that according to the diffusion theory of the lateral photoeffect [3,17] the linear dependence of lateral photovoltage on the position of the light spot is derived from a continuity equation of current of the basic carriers and presented as follows:

$$LPV = K_1 \left[e^{\beta|\varphi_i|} - 1 \right] (|x_1| - |x_2|),$$

where K_1 — coefficient of proportionality; $\beta = q/kT$; φ_i — built-in potential; $(|x_1| - |x_2|)$ — distance from the illumination point to contacts. Thus, the chief parameter which defines the value of lateral photovoltage is the height of the built-in barrier at the SiO_2/Si interface, which in turn depends on the work function of the upper layer material, which is magnetite in our case.

On the other hand, it is known [30–32] that the thin-film structures are featured with quantum-size effect, which results in an oscillating dependence of work function of the metal films on their thickness. This effect is explained by localization and quantization of a charge in the film structural elements which are comparable in sizes with the de Broglie wavelength [30,33]. It is also known [33] manifestation of the quantum-size effects in the nanomaterials is caused by the charge carriers with a small effective mass available therein, wherein in accordance with the relationship $\lambda_B = h(2m^*E)^{-1/2}$ reduction of the effective mass of electrons corresponds to the relatively high de Broglie wavelengths. For magnetite, at the room temperature the effective mass of the electron is $0.37m_0$ [34], while our calculated de Broglie wavelength (as per [31]) in

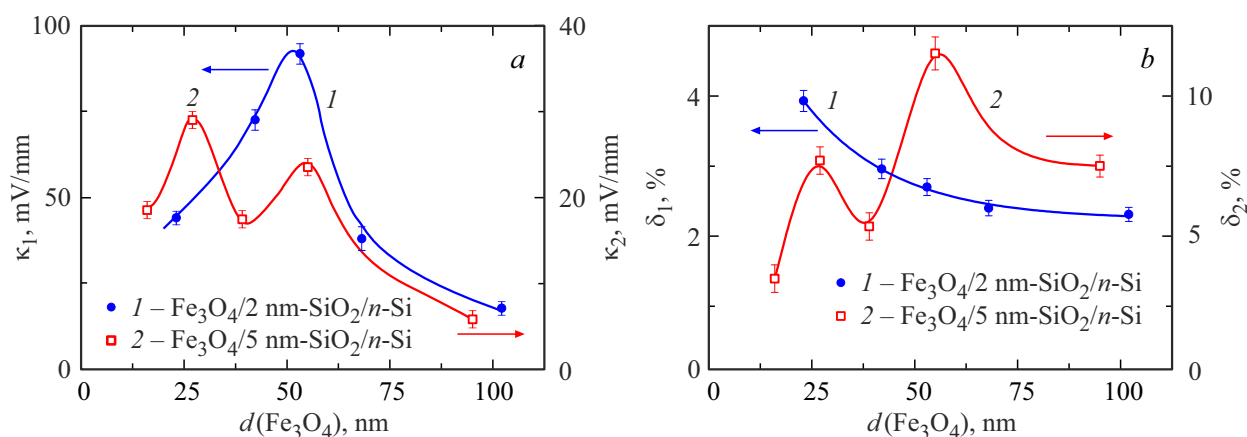


Figure 2. Thickness dependences of the LPE characteristics for the $\text{Fe}_3\text{O}_4/\text{SiO}_2/n\text{-Si}$ structures with the thickness of SiO_2 : 1 — 2 nm, 2 — 5 nm; a — LPE sensitivity $\kappa(d)$; b — LPE nonlinearity $\delta(d)$.

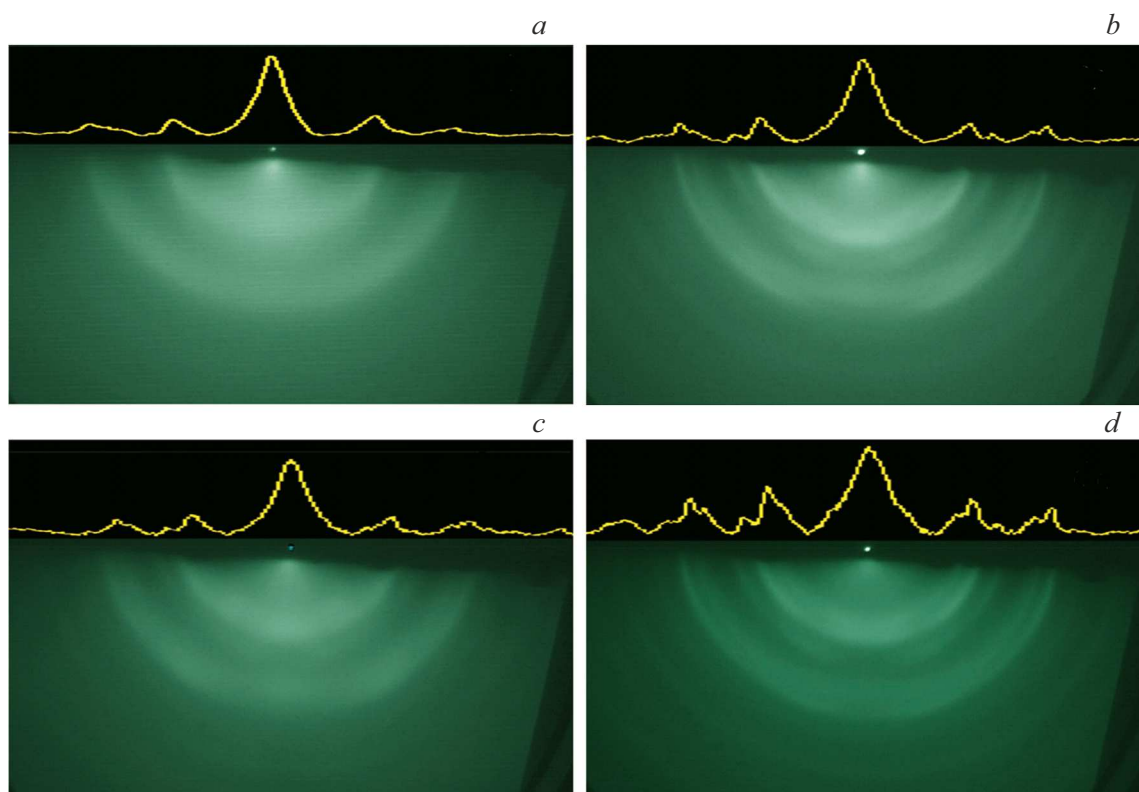


Figure 3. RHEED pattern of the $\text{Fe}_3\text{O}_4/\text{SiO}_2/n\text{-Si}$ structure a — 23nm- $\text{Fe}_3\text{O}_4/2\text{nm-SiO}_2/n\text{-Si}$; b — 27nm- $\text{Fe}_3\text{O}_4/5\text{nm-SiO}_2/n\text{-Si}$; c — 53nm- $\text{Fe}_3\text{O}_4/2\text{nm-SiO}_2/n\text{-Si}$; d — 55nm- $\text{Fe}_3\text{O}_4/5\text{nm-SiO}_2/n\text{-Si}$.

the magnetite lattice was 2.57 nm. Besides, the electronic properties of quantum-size semiconductor devices shall be referred to sizes of a structure where they are manifested. In case of layer-by-layer growth of the metal film the thickness is the only quantum-size element [30,31,35], wherein in the $\text{Fe}_3\text{O}_4/\text{SiO}_2/n\text{-Si}$ structure the upper coating is a nanocrystalline film and it is reasonable to suggest that electrons motion is quantized by the crystallite sizes. The crystallite sizes in the magnetite film were determined using a standard procedure for evaluating on RHEED patterns by

a width of the Debye rings [36]. The RHEED patterns are shown in Fig. 3, a, while the dependences of the crystallite sizes are shown on the insert of Fig. 4, a. It is found from data comparison that the maxima of LPE sensitivity correspond to structures, in which the crystallite sizes are multiples of the de Broglie wavelength. Fig. 3 shows the RHEED patterns of the $\text{Fe}_3\text{O}_4/\text{SiO}_2/n\text{-Si}$ structures for the critical thicknesses of the magnetite films. It can be seen on them that the oxidized surface of silicon has grain-oriented magnetite films growing thereon and oriented substantially

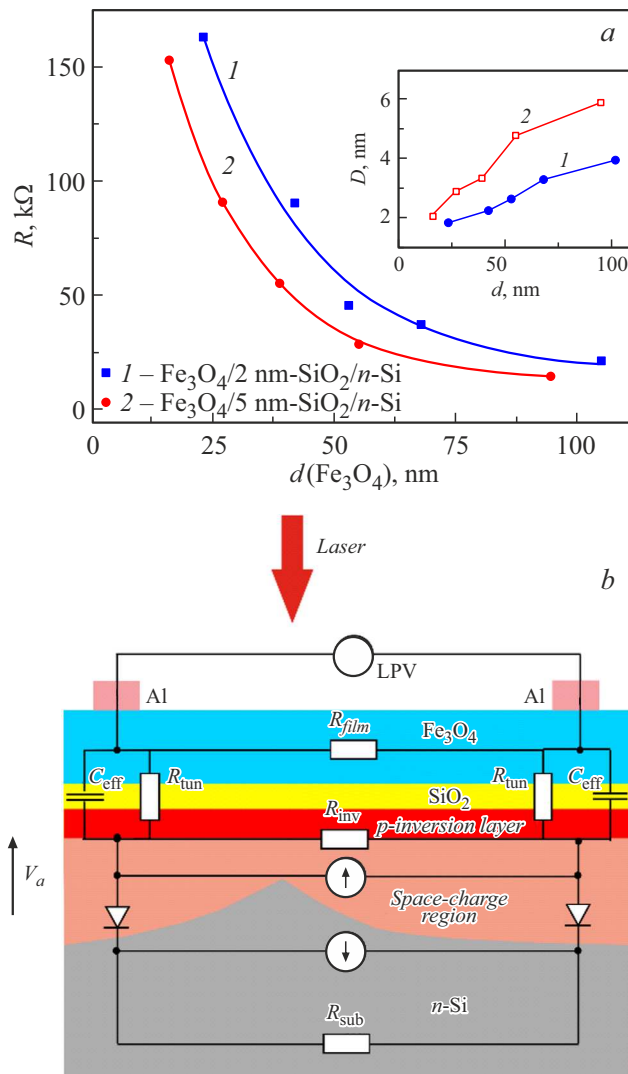


Figure 4. Transport properties of the $\text{Fe}_3\text{O}_4/\text{SiO}_2/n\text{-Si}$ structure: *a* — thickness dependences of resistance at the thickness of SiO_2 : 1 — 2 nm, 2 — 5 nm (on the insert — thickness dependences of the crystallite size); *b* — the model of lateral photoconductivity in the $\text{Fe}_3\text{O}_4/\text{SiO}_2/n\text{-Si}$ hybrid structure.

perpendicular to the surface, which is manifested as rupture of the rings on the RHEED patterns.

According to the results obtained, the ultra-thin SiO_2 layer has the Fe_3O_4 films being formed thereon and they have a lesser crystallite size (the insert of Fig. 4, *a*). One of the reasons for reduction of the crystallite size is increase of roughness of the oxidized surface of silicon in case of forming SiO_2 by wet chemical purification as compared to an isotropic surface of the thermally oxidized layer. It should be also noted here that different methods of formation of the silicon oxide layer affect the density of the interface states at the $\text{SiO}_2/n\text{-Si}$ interface, which affect the height of the built-in barrier. It is shown in the works [27,28,37] that during we chemical purification the density of the interface states is reduced. Based on that, we can assume that significant

decrease of LPE sensitivity can be related to decrease of the height of the built-in barrier due to a higher density of the interface states at the $\text{SiO}_2/n\text{-Si}$ interface as obtained by thermal oxidation.

It is known that electrophysical properties are also sensitive to a changed grain size, so it is interesting to analyze the resistance dependences of the $\text{Fe}_3\text{O}_4/\text{SiO}_2/n\text{-Si}$ structure. As can be seen in Fig. 4, *a*, for the magnetite films both on the ultra-thin (2 nm) and thin (5 nm) layer of silicon oxide as well, we have a classic curve of resistance reduction with increase of the film thickness [38] without any manifestation of the quantum-size effects. At the same time, the curve $R(d)$ for the $\text{Fe}_3\text{O}_4/\text{SiO}_2/n\text{-Si}$ structures on the ultra-thin SiO_2 layer is higher, which is a consequence of the higher density of crystallite/grain boundary and, consequently, the higher carrier scattering, which agrees with the results for the crystallite sizes as shown on the insert of Fig. 4, *a*.

However, in case of lateral photovoltage current transfer shall be analyzed taking into account the fact that the lateral photovoltage is generated in the inversion layer and the thermoelectronic emission goes from the lower level into the upper one and not vice versa as in case of resistance measurement. It has been previously shown [4,12,39] that lateral photoconductivity is realized in two parallel channels: the first one on the film (R_{film}) from which photovoltage will be taken, and the second channel — on the subsurface/inversion layer of silicon (R_{inv}) together with the near-contact regions (R_{tun}) (Fig. 4, *b*). As it is clear from Fig. 4, *a*, the thickness dependence of film resistance is of a common nature for both the structures, whereas resistance of the lower conductivity channel (R_{inv}) is determined by forming of the built-in barrier, which depends on work function of the upper coating material [40], and, therefore, its dependence on the thickness of the magnetite film will be sensitive to the quantum-size effect [31,32]. Thus, based on the assumption that with increase of the work function of Fe_3O_4 the value of the built-in potential increases as well and resistance of the inversion layer reduces, it can be concluded that the dependence $R_{\text{inv}}(d)$ will inherit the oscillating nature, though in antiphase to $\kappa(d)$.

Presence of the extrema on the dependence $R_{\text{inv}}(d)$ in the $\text{Fe}_3\text{O}_4/\text{SiO}_2/n\text{-Si}$ structure can be interpreted in terms of redistribution of channel conductivity in the two-channel model of conductivity as shown in Fig. 4, *b*. The first maximum is reached when the film becomes solid, wherein the crystallite sizes correspond to the de Broglie wavelength and the homogeneous built-in barrier is formed, while conductivity on the film becomes close to conductivity on the inversion layer of silicon. Subsequent increase of the film thickness results in various scenarios in the $\text{Fe}_3\text{O}_4/\text{SiO}_2/n\text{-Si}$ with the SiO_2 layers of the thickness 2 and 5 nm. The series with the ultra-thin SiO_2 layer exhibits only one maximum R_{inv} with the thickness of the Fe_3O_4 film 53 nm, which is related to the quantum-size effect. In the range under study we do not reach the higher crystallite sizes that are multiples of the de Broglie wavelength. Further on,

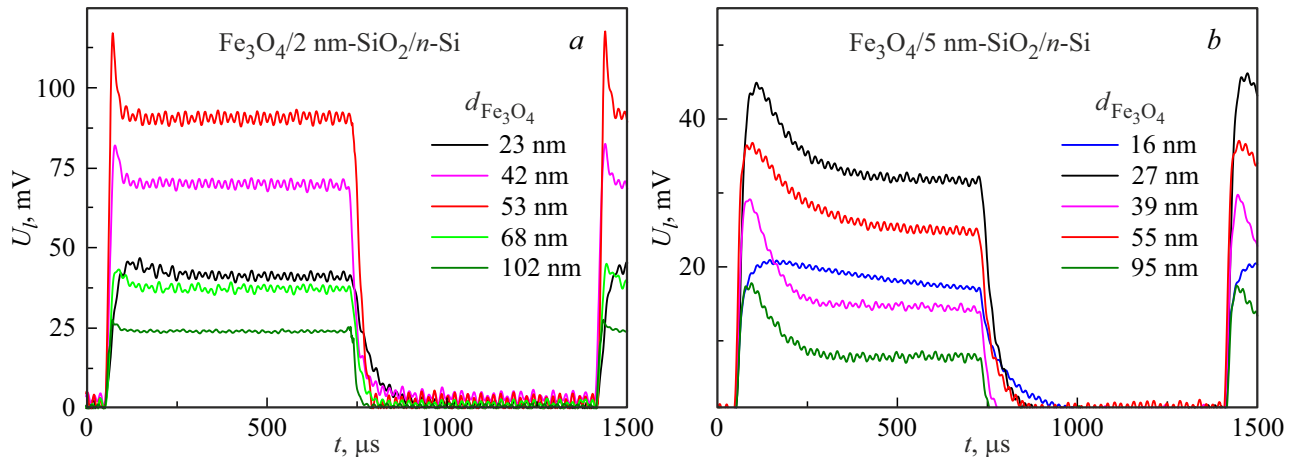


Figure 5. Pulse characteristics of the $\text{Fe}_3\text{O}_4/\text{SiO}_2/n\text{-Si}$ structure with the thickness of the SiO_2 layer: *a* — 2 nm, *b* — 5 nm.

with increase of the film thickness in this structure, its resistance significantly reduces, wherein, as noted in the literature [10,14], the channel on the film bypasses the low-lying channel, in which lateral photovoltage is generated. For the same reason, in the MOS structures on the ultra-thin SiO_2 high-resistance upper coatings are preferred [10,12]. In the series with the SiO_2 layer of the thickness of 5 nm, within the studied ranged of the thicknesses of Fe_3O_4 we have two (quantum-size) maxima of LPE sensitivity, i.e. the maximum thickness of the inversion layer is obtained twice when resistance of this layer will be the least. The „wave“ nature of changing of resistance of the inversion layer results in redistribution of photoconductivity between the channels, while the extrema correspond to switching of the conductivity channels: the maxima — switching to the channel on the film, the minimum — switching to the channel on the inversion layer. Significant reduction of lateral photovoltage in the $\text{Fe}_3\text{O}_4/5\text{nm-SiO}_2/n\text{-Si}$ structure is also related to more significant voltage drop in the near-contact regions (RC-circuit under pulsed illumination and its active part under continuous illumination).

Thus, the two conductivity channels — the upper one on the film and the lower one on the inversion layer — function in the superposition mode, while their contributions are redistributed when conductivity on one of the channels starts prevailing as a result of competition.

So, as a result of changing of the parameters of the multi-layer $\text{Fe}_3\text{O}_4/\text{SiO}_2/n\text{-Si}$ structure, in particular, increasing the thickness of the SiO_2 buffer layer, the dependences $R_{inv}(d)$, $\kappa(d)$ and $\delta(d)$ have the multi-mode nature, which is not typical for the MOS structures based on the ultra-thin SiO_2 . It is related to manifestation of the quantum-size effect in the magnetite film, which has in the structure based on the 5nm- $\text{SiO}_2/n\text{-Si}$ a larger crystallite size, which in our study is doubly multiple of the de Broglie wavelength in the magnetite.

It is also interesting to study LPE in the $\text{Fe}_3\text{O}_4/\text{SiO}_2/n\text{-Si}$ under pulsed illumination, as it is transition characteristics

that will be the most sensitive to parameters of the RC filters in the near-contact regions. Fig. 5 shows time dependences of lateral photovoltage in the $\text{Fe}_3\text{O}_4/\text{SiO}_2/n\text{-Si}$ (001) structure under local illumination of the near-contact region with laser with the wavelength of 633 nm and the frequency of the light pulses of 737 Hz. By comparing Fig. 5, *a* and *b*, it can be seen that the photoresponse signals on the ultra-thin and the thin SiO_2 layer differ not only in the value of the pulse amplitude, but in their form as well.

As can be seen in Fig. 5, the photoresponse signal amplitude corresponds to the value of LPE sensitivity (Fig. 2, *a*). As stated in the work [41], the form of the photoresponse signal depends on the number of the photogenerated electron-hole pairs that are separated at the $\text{SiO}_2/n\text{-Si}$ interface. It follows from the analysis of Fig. 5 that the structure based on the ultra-thin SiO_2 generates more electron-hole pairs, in several orders of the magnitude, as compared with the structure based on the thermally oxidized SiO_2 layer. As shown above, reduction of the number of the electron-hole pairs in the $\text{Fe}_3\text{O}_4/\text{SiO}_2/n\text{-Si}$ structure formed on the thermally oxidized surface of silicon is caused by reduction of the height of the built-in barrier due to increase of the density of the interface states at the interface. $\text{SiO}_2/n\text{-Si}$.

The table shows the times of rising and falling of the photoresponse signals in the $\text{Fe}_3\text{O}_4/\text{SiO}_2/n\text{-Si}$ structures which have the highest LPE sensitivity in Fig. 2, *a*. The times of rising (t_r) and falling (t_f) of the photoresponse signals are defined as the time required to increase the photoresponse from 10% to 90% of the photoresponse peak and the time required to reduce the photoresponse from 90% to 10%, respectively [42]. Besides, the constants of the time of rising (τ_r) and falling (τ_f) were defined using a Boltzman sigmoidal function and the exponential function, respectively. The data of the table indicate that increase of the thickness of the SiO_2 layer resulted in increase of the falling time of the photoresponse curves, which is related to increase of tunneling resistance (Fig. 4, *b*). Thus, under

Time parameters of the photoresponse in the structure $\text{Fe}_3\text{O}_4/\text{SiO}_2/n\text{-Si}$

Parameters of the structure	$t_r, \mu\text{s}$	$t_f, \mu\text{s}$	$\tau_r, \mu\text{s}$	$\tau_f, \mu\text{s}$
27nm- $\text{Fe}-3\text{O}_4/5\text{nm-SiO}_2/\text{Si}$	17.8 ± 0.5	126 ± 1	5.3 ± 0.1	36.5 ± 0.3
55nm- $\text{Fe}_3\text{O}_4/5\text{nm-SiO}_2/\text{Si}$	13.3 ± 0.3	112 ± 7	3.6 ± 0.1	35.2 ± 0.5
53nm- $\text{Fe}_3\text{O}_4/2\text{nm-SiO}_2/\text{Si}$	14.0 ± 0.3	49 ± 5	3.5 ± 0.1	20.5 ± 0.3

pulsed illumination changing of the parameters of the buffer layer of the $\text{Fe}_3\text{O}_4/\text{SiO}_2/n\text{-Si}$ structure results in changing both of the characteristics of the RC-circuit in the near-contact regions and the number of the electron-hole pairs generated in the illuminated region at the SiO_2/Si interface.

Conclusion

With all the obviousness of the advantage of the $\text{Fe}_3\text{O}_4/\text{SiO}_2/n\text{-Si}$ structure based on the ultra-thin SiO_2 , the present research is not only of practical interest, but also of fundamental interest for understanding the mechanism of lateral photoconductivity in the MOS structures. It is shown that the work function of the Fe_3O_4 film, the height of the built-in barrier at the SiO_2/Si interface and electrical resistance of the inversion layer in the $\text{Fe}_3\text{O}_4/\text{SiO}_2/n\text{-Si}$ structure are defined by the surface and interface states at the SiO_2/Si interface, which depend on the method of silicon surface oxidation. It is noted that on the thermally oxidized surface of silicon the work function of Fe_3O_4 has the oscillating dependence with increase of the film thickness, which is related to the sizes of the magnetite nanocrystals. It has been established that the maximum LPE sensitivity is reached with predominant conductivity of the inversion layer channel in the two-channel model of lateral photoconductivity, when the magnetite crystallite sizes are multiples of de Broglie wavelength. It is shown that under pulsed illumination of the $\text{Fe}_3\text{O}_4/\text{SiO}_2/n\text{-Si}$ structure the transition processes in the RC-circuit related to changing of the thickness of the SiO_2 layer will affect the time characteristics of the photoresponse, while the generation & recombination processes due to the value of the built-in potential will affect the form of the photoresponse signal.

Acknowledgments

The authors would like to thank V.V. Korobtsov for consulting on this topic and A.A. Dimitriev for help in assembling and calibrating the optical plant.

Funding

The present study was funded by the budget of Institute of Automation and Control Processes of Far Eastern Branch of RAS under state assignment (the subject № FFWF-2021-0002).

Conflict of interest

The authors declare that they have no conflict of interest.

References

- [1] J.T. Wallmark. Proc. IRE, **45** (4), 474 (1957). DOI: 10.1109/JRPROC.1957.278435
- [2] G. Lucovsky. J. Appl. Phys., **31** (6), 1088 (1960). DOI: 10.1063/1.1735750
- [3] P.P. Konorov, Yu.A. Tarantov. Uchenye zapiski LGU, Ser. fizicheskikh nauk, **370** (17), 114 (1974). (in Russian)
- [4] T. Shikama, H. Niu, M. Takai. Jpn. J. Appl. Phys., **23** (10R), 1314 (1984). DOI: 10.1143/JJAP.23.1314
- [5] A. Samarin. Elektronnye komponenty, **7**, 103 (2003). (in Russian)
- [6] W.C. Ma, A.A. Rizzi, R.L. Hollis. Proc. 2000 ICRA. Millennium Conference. IEEE International Conference on Robotics and Automation. Symposia Proceedings (Cat. No. 00CH37065). V. 2. IEEE, 2000). DOI: 10.1109/ROBOT.2000.844828
- [7] E. Fortunato, G. Lavareda, R. Martins, F. Soares, L. Fernandes. Sens. Actuators A: Phys., **51** (2–3), 135 (1995). DOI: 10.1016/0924-4247(95)01214-1
- [8] J. Henry, J. Livingstone. J. Phys. D: Appl. Phys., **41** (16), 165106 (2008). DOI: 10.1088/0022-3727/41/16/165106
- [9] W. Wang, J. Lu, Z. Ni. Nano Res., **14**, 1889 (2021). DOI: 10.1007/s12274-020-2917-3
- [10] C. Yu, H. Wang. Sensors, **10** (11), 10155 (2010). DOI: 10.3390/s101110155
- [11] S. Qiao, B. Liang, J. Liu, G. Fu, S. Wang. J. Phys. D: Appl. Phys., **54** (15), 153003 (2021). DOI: 10.1088/1361-6463/abd433
- [12] T.A. Pisarenko, V.V. Korobtsov, A.A. Dimitriev, V.V. Balashev. Physics Solid State, **64** (8), 1111 (2022). DOI: 10.21883/PSS.2022.08.54635.363
- [13] H. Nguyen, A.R.M. Faisal, T. Nguyen, T. Dinh, E.W. Streed, N.T. Nguyen, D.V. Dao. J. Phys. D: Appl. Phys., **54** (26), 265101 (2021). DOI: 10.1088/1361-6463/abf3ff
- [14] J. Dai, L. Spinu, K.Y. Wang, L. Malkinski, J. Tang, J. Phys. D: Appl. Phys., **33** (11), L65 (2000). DOI: 10.1088/0022-3727/33/11/101
- [15] W.B. Mi, E.Y. Jiang, H.L. Bai. J. Appl. Phys., **107** (10), 103922 (2010). DOI: 10.1063/1.3429082
- [16] V.A. Vikulov, A.A. Dimitriev, V.V. Balashev, T.A. Pisarenko, V.V. Korobtsov. Mater. Sci. Eng., **B 211**, 33 (2016). DOI: 10.1016/j.mseb.2016.05.014
- [17] T.A. Pisarenko, V.V. Balashev, V.A. Vikulov, A.A. Dimitriev, V.V. Korobtsov. Physics Solid State, **60**, 1316 (2018). DOI: 10.1134/S1063783418070223]

- [18] T.A. Pisarenko, V.V. Korobtsov, V.V. Balashev, A.A. Dimitriev, S.V. Bondarenko. *Solid State Phenom.*, **312**, 98 (2020). DOI: 10.4028/www.scientific.net/SSP.312.98
- [19] T.A. Pisarenko, V.V. Korobtsov, V.V. Balashev, A.A. Dimitriev. *Solid State Phenom.*, **312**, 92 (2020). DOI: 10.4028/www.scientific.net/SSP.312.92
- [20] T.A. Pisarenko, V.V. Balashev, V.V. Korobtsov, A.A. Dimitriev. *Defect Diffus. Forum*, **386**, 137 (2018). DOI: 10.4028/www.scientific.net/DDF.386.137
- [21] V.V. Shchennikov, S.V. Ovsyannikov. *J. Phys.: Condens. Matter.*, **21** (27), 271001 (2009). DOI: 10.1088/0953-8984/21/27/271001
- [22] F. Walz. *J. Phys.: Condens. Matter.*, **14** (12), R285 (2002). DOI: 10.1088/0953-8984/14/12/203
- [23] H. Kobayashi, Asuha, O. Maida, M. Takahashi, H. Iwasa. *J. Appl. Phys.*, **94** (11), 7328 (2003). DOI: 10.1063/1.1621720
- [24] Y. Ishizaka, J. Shiraki. *Electrochem. Soc.*, **133** (4), 666 (1986). DOI: 10.1149/1.2108651
- [25] N.F. Mott, S. Rigo, F. Rochet, A.M. Stoneham. *Philos. Mag. B*, **60** (2), 189 (1989). DOI: 10.1080/1364281890821119
- [26] H.Z. Massoud, J.D. Plummer, E.A. Irene. *J. Electrochem. Soc.*, **132** (11), 2685 (1985). DOI: 10.1149/1.2113648
- [27] T. Matsumoto, H. Nakajima, D. Irishika, T. Nonaka, K. Imamura, H. Kobayashi. *Appl. Surf. Sci.*, **395**, 56 (2017). DOI: 10.1016/j.apsusc.2016.06.001
- [28] H. Fukuda, M. Yasuda, T. Iwabuchi, S. Kaneko, T. Ueno, I. Ohdomari. *J. Appl. Phys.*, **72** (5), 1906 (1992). DOI: 10.1063/1.351665
- [29] J. Shewchun, D. Burk, M.B. Spitzer. *IEEE Trans. Electron Devices*, **27** (4), 705 (1980). DOI: 10.1109/T-ED.1980.19926
- [30] F.K. Schulte. *Surf. Sci.*, **55** (2), 427 (1976). DOI: 10.1016/0039-6028(76)90250-8
- [31] C. Li, W. Chen, M. Li, Q. Sun, Y. Jia. *New J. Phys.*, **17** (5), 053006 (2015). DOI: 10.1088/1367-2630/17/5/053006
- [32] F. Lavini, A. Caló, Y. Gao, E. Albisetti, T. Cao, G. Li, C. Aruta, E. Riedo. *Nanoscale*, **10** (17), 8304 (2018). DOI: 10.1039/RG.2.2.29012.45445
- [33] N.D. Zhukov, V.F. Kabanov, A.I. Mihaylov, D.S. Mosiyash, Ya.E. Pereverzev, A.A. Hazanov, M.I. Shishkin. *Semiconductors*, **52**, 78 (2018). DOI: 10.1134/S1063782618010256
- [34] S. Taketomi, H. Takahashi, N. Inaba, H. Miyajima. *J. Phys. Soc. Jpn.*, **60** (10), 3426 (1991). DOI: 10.1143/JPSJ.60.3426
- [35] X. Liu, S.B. Zhang, X.C. Ma, J.F. Jia, Q.K. Xue, X.H. Bao, W.X. Li. *Appl. Phys. Lett.*, **93** (9), 093105 (2008). DOI: 10.1063/1.2977529
- [36] J.T. Drotar, T.M. Lu, G.C. Wang. *J. Appl. Phys.*, **96** (12), 7071 (2004). DOI: 10.1063/1.1811785
- [37] L.B. Freeman, W.E. Dahlke. *Solid-State Electron.*, **13** (11), 1483 (1970). DOI: 10.1016/0038-1101(70)90084-5
- [38] E.H. Sondheimer. *Adv. Phys.*, **50** (6), 499 (2001). DOI: 10.1080/00018730110102187
- [39] X. Wang, B. Song, M. Huo, Y. Song, Z. Lv, Y. Zhang, Y. Wang, Y. Song, J. Wen, Y. Sui. *J. Tang, RSC Adv.*, **5** (80), 65048 (2015). DOI: 10.1039/C5RA11872G
- [40] A.M. Cowley, S.M. Sze. *J. Appl. Phys.*, **36** (10), 3212 (1965). DOI: 10.1063/1.1702952
- [41] A.E. Iverson, D.L. Smith. *IEEE Trans. Electron Devices*, **34** (10), 2098 (1987). DOI: 10.1109/T-ED.1987.23203
- [42] W.S. Levine. *The control handbook* (Jaico Publishing House, Mumbai, 1999), v. 1, p. 158.

Translated by M. Shevelev